2

ROASTING OF SULFIDE MINERALS

In addition to common metals like copper, lead, zinc, and nickel a number of other metals such as antimony, bismuth, cadmium, cobalt, mercury, and molybdenum occur as sulfide minerals. Sulfides are not reduced with the most widely used reducing agents, carbon and hydrogen, because the free energy change for the reactions $2MS + C = 2M + CS_2$ and $MS + H_2 = M + H_2S$ is positive due to the lesser stability of CS_2 and H_2S, compared to most sulfides. Reduction of sulfides with metals is not economical. Furthermore, from most sulfide minerals the metal value is not brought into aqueous solution by leaching with common acids and alkalis. In the presence of an oxidant, chalcocite is leached quickly in dilute sulfuric acid whereas bornite and covellite are leached slowly. Leaching is speeded up in the presence of bacteria. But chalcopyrite, the major source of copper is not leached. Commercially, pentlandite, a nickel sulfide mineral, is treated with ammonia under pressure (8 atm) at 105°C to dissolve nickel. Nickel is precipitated by blowing hydrogen at 30 atm in the purified leach liquor at 170°C. Otherwise, by and large, the hydrometallurgical route for treatment of sulfides has failed. Under the circumstances, the only alternative seems to be the conversion of sulfide concentrates into oxides by dead roasting [1–3], which can be easily reduced with carbon (production of lead and zinc) or into mixed oxide and sulfate by partial roasting and sintering, which can be dissolved in dilute sulfuric acid and the resultant solution is subjected to electrowinning (extraction of zinc).

Until the very recent past, roasting happened to be a preliminary chemical treatment in the extraction of copper from chalcopyrite via the pyrometallurgical route incorporating steps, namely, concentration by froth flotation, reverberatory smelting,

---

Physical Chemistry of Metallurgical Processes, First Edition. M. Shamsuddin.

converting, fire refining, and electrorefining. Although 80% of the total world production of copper comes from the chalcopyrite concentrate even today, the roasting step has been eliminated from the flow sheet on account of recently developed faster smelting and converting processes, for example, flash smelting by the International Nickel Company and Outokumpu, submerged tuyere smelting by Noranda and Teniente, Ausmelt/Isasmelt matte smelting, continuous converting by Outokumpu and Mitsubishi, and direct smelting/converting by Mitsubishi. The roasting is also eliminated in the production of lead from galena concentrate by the Ausmelt process. However, roasting plays an important role in the extraction of nickel from pentlandite, zinc from sphalerite, and molybdenum from molybdenite.

In roasting, air in large amounts, sometimes enriched with oxygen, is brought into contact with the sulfide mineral concentrate. This is done at elevated temperatures when oxygen combines with sulfur to form sulfur dioxide and with the metal to form oxides, sulfates and so on. The oxidation must be done without melting the charge in order to prevent reduction of particle surface–oxidizing gas contact area. Stirring of the charge in some manner also ensures exposure of all particle surfaces to the oxidizing gas. Exception to this procedure is blast roasting-sintering, where the particle surfaces are partially melted and there is no stirring of the charge. The degree of sulfur elimination is controlled by regulating the air supply to the roaster and by the degree of affinity of the mineral elements for sulfur or oxygen. For example, iron sulfide may all be oxidized because iron has more affinity for oxygen than for sulfur, while a copper mineral in the same roaster feed will emerge in the calcine still as a sulfide due to greater affinity of copper for sulfur than for oxygen.

Roasting is essentially a surface reaction where the oxide layer is formed first and continues to remain as a porous layer through which oxygen can pass into the still unreacted inner sulfide portion of the particle and the SO_2 gas formed comes out. Roasting is an exothermic reaction. This heat helps to keep the roaster at the required roasting temperature so that the process can continue with little extra heat supplied by the burning fuel. Hence, sulfide roasting is an autogenous process, that is, where no extra fuel is supplied.

2.1 METHODS OF ROASTING

There are several commercial roasters used on the industrial scale. The multiple hearth roaster that consists of a number of horizontal circular refractory hearths placed one above the other in a steel shell for the purpose of charging the feed on the top hearth as well as for discharging the roasted calcine from the bottom hearth, has been virtually replaced by the flash or suspension roaster that has only the top and bottom hearths. The capacity of such roasters is three times larger than that of multiple hearth roasters. In flash roasting, the preheated ore is injected through a burner. This process is most appropriate for the roasting of sulfides, which oxidize exothermally and require no additional fuel. In flash roasting, the benefits of a counter flow operation are partially lost.

The use of fluidized beds for roasting fine concentrate is obviously attractive. If a gas is passed upward through a bed of solid particles of small and preferably regular size in the range 2–0.02 mm diameter, the behavior of the bed will depend upon the velocity of the gas. At very low flow rates the gas permeates through the bed without moving the particles at all and the pressure drop across the bed is proportional to the flow rate. An increase in gas velocity to a critical value causes the bed to expand as the effective weights of the particles become balanced by the drag forces of the gas stream upon them. Over a short range of velocities, the particles remain individually suspended, each with a downward velocity relative to the gas stream approximately equal to its terminal velocity.

Ore fines may be sintered due to incipient fusion in Dwight Lloyd Sintering Machine. It consists of a linked grate section, which forms an endless belt that moves on rollers. A suction box is located under the grate and the speed of the belt movement is adjusted.

2.2 OBJECTIVES

In the extraction of metals from sulfides, roasting is applied to achieve different objectives depending on the overall process flow sheet. Such objectives include one or more of the following:

Oxidizing roast is carried out to prepare a totally or a partly oxide product. For example, dead roasting of sphalerite concentrate to an all oxide product is the prerequisite for the pyrometallurgical smelting processes. For copper and nickel extraction only partial roasting is practiced. In order to produce a mixed oxide-sulfate product *Sulfation roast* is preferred. The most outstanding example of this is found in the commercial production of zinc by the hydrometallurgical route. *Roast-reduction* is aimed at producing a metal directly by the interaction between the oxide formed *in situ* and the unroasted sulfide. This is employed in the old and now obsolete “Newnam Ore Hearth Process” of making lead. Such a principle is also partially made use of in the sintering (agglomeration) of galena concentrates. The objective of *Chloridizing roast* is to convert certain metals to their water soluble chlorides. Notable among such applications is the treatment of pyrite cinders with $CaCl_2$ for the recovery of nonferrous values. *Volatilizing roast* is used to produce and recover metals as volatile oxides or for the elimination of unwanted metals as volatilized oxides. Roasting of speiss for As_2O_3 recovery and of bismuth ores for the removal of As, Sb or Zn (as their oxides) are very interesting applications under this category.

Obviously, roasting is a very vast field with multifarious aspects covering the fundamental, applied, and industrial aspects of many metal sulfides. It would not be possible to survey the whole field with any justice. However, it would be interesting to discuss the relevant chemistry and thermodynamics of roasting with the primary aim of understanding the stability regions of different phases in M—S—O systems in the following sections.

2.3 CHEMISTRY OF ROASTING

The chemistry of sulfide roasting is complex involving numerous reactions, important of which are as follows:

1. Decomposition of higher sulfides to lower sulfides, for example,

$$MS_2(s) = MS(s) + \frac{1}{2}S_2(g) \tag{2.1}$$

$$2MS_2(s) = M_2S_3(s) + \frac{1}{2}S_2(g) \tag{2.2}$$

2. Oxidation of sulfides to form oxides or sulfates

$$2MS(s) + 3O_2(g) = 2MO(s) + 2SO_2(g) \tag{2.3}$$

$$MS(s) + 2O_2(g) = MSO_4(s) \tag{2.4}$$

3. Burn-up of sulfur to form its oxides

$$S_2(g) + 2O_2(g) = 2SO_2(g) \tag{2.5}$$

$$2SO_2(g) + O_2(g) = 2SO_3(g) \tag{2.6}$$

4. Sulfation of metal oxides

$$MO(s) + SO_3(g) = MSO_4(s) \tag{2.7}$$

$$2MO(s) + 2SO_2(g) + O_2(g) = 2MSO_4(s) \tag{2.8}$$

5. Decomposition of sulfates to basic (oxy) sulfates

$$2MSO_4(s) = MO{\cdot}MSO_4(s) + SO_3(g) \tag{2.9}$$

$$MO{\cdot}MSO_4(s) = 2MO(s) + SO_3(g) \tag{2.10}$$

$$MSO_4(s) = MO{\cdot}ySO_3(s) + (1-y)SO_3(g) \tag{2.11}$$

6. Sulfide–sulfate interaction

$$MS(s) + 3MSO_4(s) = 4MO(s) + 4SO_2(g) \tag{2.12}$$

7. Sulfide–oxide interaction

$$MS(s) + 2MO(s) = 3M(s) + SO_2(g) \tag{2.13}$$

8. Reaction between product oxides or product and impurity oxides to form complex compounds such as ferrites and silicates

$$2MO(s) + 2FeO(s) = 2MFeO_2(s) \tag{2.14}$$

$$2MO(s) + SiO_2(s) = M_2SiO_4(s) \tag{2.15}$$

9. Formation of sub- or higher-oxides

$$2MO(s) = M_2O(s) + \frac{1}{2}O_2(g) \tag{2.16}$$

$$2MO(s) + \frac{1}{2}O_2(g) = M_2O_3(s) \tag{2.17}$$

10. Other reduction or oxidation reactions such as

$$3M_3O_4(s) + MS(s) = 10MO(s) + SO_2(g) \tag{2.18}$$

$$M(s,l) + SO_2(g) = MS(s) + O_2(g) \tag{2.19}$$

Where more than one metal sulfide is present in the concentrate, the reactions are truly complex and very large in number. The composition of a product in sulfide roasting depends not only on the chemical and mineralogical composition of the concentrate, temperature, and partial pressures of O_2, SO_2, and SO_3 but also on the other process parameters such as particle size, mixing, time of reaction, and the technique of roasting.

2.4 THERMODYNAMICS OF ROASTING

The necessary conditions for the formation of different products can be illustrated by the relationship between the equilibriums in any M—S—O system. In the simplest case we have three components and according to the phase rule ($P = C - F + 2$) there can be five phases, that is, four condensed phases and one gaseous phase ($P = 3 - 0 + 2 = 5$). P, C and F respectively stand for the number of phases, components and degree of freedom. If temperature is fixed, we have $P = 3 - 0 + 1 = 4$ (3 condensed phases and 1 gaseous phase). The gas phase normally contains SO_2 and O_2 but some SO_3 and even sulfur vapor (S_2) may be present. Among the gaseous compounds the following equilibria exist:

$$S_2(g) + 2O_2(g) = 2SO_2(g) \tag{1}$$

$$2SO_2(g) + O_2(g) = 2SO_3(g) \tag{2}$$

At any selected temperature the composition of the gas mixture is defined by the partial pressures of two of the gaseous components. Further, for any fixed gas composition,

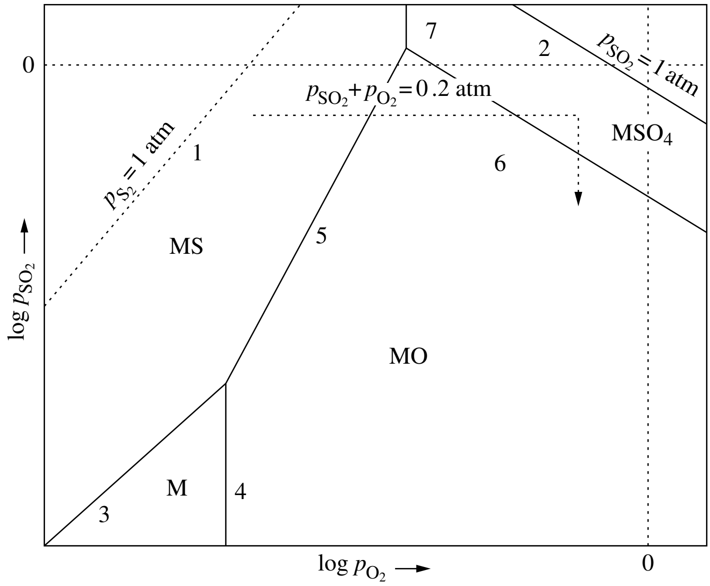

FIGURE 2.1 Predominance area diagram of the M—S—O system (From Principles of Extractive Metallurgy by T. Rosenqvist [3], © 1974, p 247, McGraw-Hill Inc. Reproduced with the permission of McGraw-Hill Book Co.).

the composition of the condensed phase gets fixed. Thus, the phase relationship in the ternary system at constant temperature may be described in a two-dimensional diagram, where the two co-ordinates are the partial pressures of two of the gaseous components, when generally, p_{SO_2} and p_{O_2} are chosen. Such isothermal plots are called Predominance Area Diagrams. They are also known as Kellogg Diagrams [4–6], after Kellogg, who conceived them. Commencing with the pioneering and innovative work of Kellogg and his co-workers, several researchers have constructed the predominance area diagrams not only for M—S—O systems but also for M_1—M_2—S—O systems. Many such diagrams are available in literature [7–15] and have been made use of to understand roasting, decomposition, smelting, refining, and so on.

Figure 2.1 shows equilibria and predominance areas at a constant temperature for the M—S—O system. Lines describing the equilibrium between any two condensed phases are given by equations:

$$M(s) + SO_2(g) = MS(s) + O_2(g) \tag{3}$$

$$2M(s) + O_2(g) = 2MO(s) \tag{4}$$

$$2MS(s) + 3O_2(g) = 2MO(s) + 2SO_2(g) \tag{5}$$

$$2MO(s) + 2SO_2(g) + O_2(g) = 2MSO_4(s) \tag{6}$$

$$MS(s) + 2O_2(g) = MSO_4(s) \tag{7}$$

If metal forms several sulfides and oxides, additional equilibria would have to be considered for the formation of MS_2, M_2O_3 and $M_2(SO_4)_3$ and so on. In addition, basic sulfates, $MO{\cdot}MSO_4$ may exist. For the above reactions for all condensed phases in their standard states, the equilibria are given by the expressions:

$$K_3 = \frac{a_{MS}\cdot p_{O_2}}{a_M\cdot p_{SO_2}} = \frac{p_{O_2}}{p_{SO_2}} \quad \text{i.e., } \log p_{O_2} - \log p_{SO_2} = \log K_3$$

$$K_4 = \frac{1}{p_{O_2}} \quad \text{i.e., } \log p_{O_2} = -\log K_4$$

$$K_5 = \frac{p^2_{SO_2}}{p^3_{O_2}} \quad \text{i.e., } -3\log p_{O_2} + 2\log p_{SO_2} = \log K_5$$

$$K_6 = \frac{1}{p^2_{SO_2} p_{O_2}} \quad \text{i.e., } \log p_{O_2} + 2\log p_{SO_2} = -\log K_6$$

$$K_7 = \frac{1}{p^2_{O_2}} \quad \text{i.e., } 2\log p_{O_2} = -\log K_7$$

We notice that for a given reaction the form of the equilibrium expression is the same for all metals, that is, the slope of the corresponding lines in the figure is the same. Only the values of the equilibrium constant K_3, K_4, and so on, may differ from one metal to another. This means that the position of the equilibrium lines may change and, consequently, the size and the position of the areas between the lines. These areas are called the predominance area for that particular phase. From the figure we find that

1. As long as only one condensed phase exists, the partial pressure of SO_2 and O_2 may be changed independently of each other; that is, the system at constant temperature has two degrees of freedom.
2. Along the lines for equilibrium between two condensed phases, the system has one degree of freedom.
3. Finally, where three phases are in equilibrium, the system at constant temperature is nonvariant.

There are also lines in the figure to describe reactions (1) and (2) that is, for the formation of SO_2 and SO_3. These are given by the expressions:

$$K_1 = \frac{p^2_{SO_2}}{p_{S_2}\cdot p^2_{O_2}} \quad \text{i.e., } 2\log p_{SO_2} - 2\log p_{O_2} = \log K_1 + \log p_{S_2}$$

$$K_2 = \frac{p^2_{SO_3}}{p^2_{SO_2}\cdot p_{O_2}} \quad \text{i.e., } 2\log p_{SO_2} + \log p_{O_2} = -\log K_2 + 2\log p_{SO_3}$$

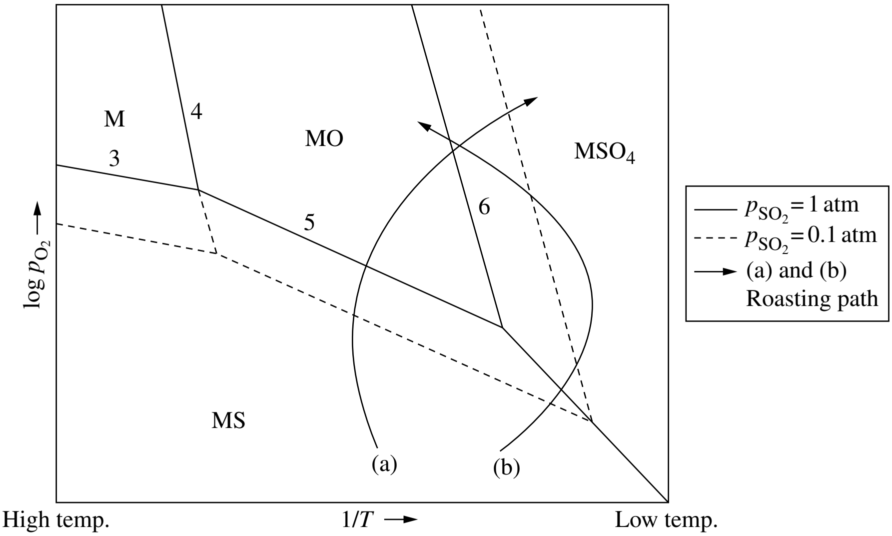

FIGURE 2.2 Effect of temperature on equilibria and predominance areas in the M—S—O system at constant pressure of SO_2 gas (From Principles of Extractive Metallurgy by T. Rosenqvist [3], © 1974, p 250, McGraw-Hill Inc. Reproduced with the permission of McGraw-Hill Book Co.).

This means that for fixed values of K_1 and K_2, the relationship between $\log p_{SO_2}$ and $\log p_{O_2}$ depends also on the partial pressures of S_2 and SO_3. In the figure the lines are drawn for $p_{S_2} = 1$ atm and $p_{SO_3} = 1$ atm. For other pressures the lines are to be shifted up and down in accordance with the above expressions. Thus, p_{S_2} becomes large when p_{O_2} is small and that p_{SO_2} is large and p_{SO_3} is large for large values of p_{SO_2} and p_{O_2}. When roasting is carried out in air, $p_{SO_2} + p_{O_2} = 0.2$ atm, the conditions during roasting are as described by the dotted lines in the figure. First, the sulfide is roasted/converted into the oxide by reaction (5). Then the oxide may be converted into sulfate, which by prolonged heating in air at constant temperature again may be converted to give the oxide.

Since the predominance areas for different metals have different locations [3], the reactions for a mixed sulfide ore will not occur simultaneously for the different metals, and some reactions may not occur at all. Thus, for mixed Cu—Fe sulfide, iron sulfide will first oxidize to form Fe_3O_4. Copper will then still be present as Cu_2S. Further, oxidation converts Fe_3O_4 into Fe_2O_3 and Cu_2S into Cu_2O and further into CuO. The effect of temperature on the roasting equilibria may be given in a two-dimensional diagram for constant values of p_{SO_2}. The Figure 2.2 shows $\log p_{O_2}$ vs $1/T$ plots for $p_{SO_2} = 1$ atm and 0.1 atm. Slope of the curves giving enthalpy of the reaction is expressed in terms of 1 mol of oxygen:

$$\mathrm{M(s)} + \mathrm{SO_2(g)} = \mathrm{MS(s)} + \mathrm{O_2(g)}, \quad K_3 = \frac{p_{O_2}}{p_{SO_2}}$$

For a fixed value of p_{SO_2}: $\dfrac{\partial \log p_{O_2}}{\partial(1/T)} = \dfrac{\partial \log K_3}{\partial(1/T)} = \dfrac{\Delta H_3}{4.575}$

In Figure 2.2, two possible roasting paths have been marked. Normally, with increase of temperature sulfide gets roasted to oxide along the path shown by the curve (a). Toward the end of the roasting process when temperature falls, some sulfate may be formed. In the second case presented by the curve (b), during roasting, first the sulfate is formed at low temperature. If temperature increases by means of additional heat it decomposes to oxide. In the above discussion, reactions for only one metal sulfide independent of other metals have been considered but in roasting of complex sulfide ores many additional reactions may occur. Different sulfides may form solid solutions as well as complex sulfides. Further, oxides formed may give rise to the formation of complex oxides. For example, the roasted product of chalcopyrite, $CuFeS_2$, may consist of a number of ternary phases and also solid solution of FeS and Cu_2S.

On the other hand, in roasting of sphalerite, zinc ferrite ($ZnO{\cdot}Fe_2O_3$) is formed due to the presence of iron oxide as a gangue in the concentrate. Depending on the temperature of roasting oxy-sulfates like $ZnO{\cdot}ZnSO_4$ and $PbO{\cdot}PbSO_4$, $PbO{\cdot}2PbSO_4$, and $PbO{\cdot}4PbSO_4$ are formed in roasting of sphalerite and galena, respectively. The shape and extent of stability regions alter when such complex phases are formed because the activity of the compound in the complex phase is less than the activity of the pure compound. Thus, zinc ferrite will be formed from sphalerite at a partial pressure of oxygen lower than what zinc oxide formation would require. Similarly, higher partial pressures of oxygen and sulfur dioxide will be required for ZnO—$ZnSO_4$ equilibrium if ZnO is bonded in a ferrite phase as compared to its presence as pure ZnO.

Predominance area diagrams at different temperatures for different M—S—O systems are useful in carrying out selective roasting depending on the requirement of the process flow sheets. This is illustrated in the preparation of different types of feed for the reverberatory smelting and leaching circuit by roasting chalcopyrite (though not practiced currently but helpful in assessing the usefulness of such diagrams) with the aid of stability diagrams of Cu—S—O and Fe—S—O. Predominance area diagrams of Cu—S—O, Fe—S—O, Zn—S—O and Pb—S—O have been made use of effectively to demonstrate the possibility of selective roasting of an off-grade chalcopyrite concentrate [13] containing appreciable amounts of sphalerite and galena (see problem 2.6).

2.5 KINETICS OF ROASTING

Roasting of sulfides, in general, is exothermic and hence the temperature of the ore lump remains high enough for the desired chemical reactions to occur fairly early during the roasting process. Every particle gets oxidized from the outside, which leads to the formation of a case of solid product and leaves a core of unchanged zone. The required reaction occurs at the interface between these zones if the gas ratio p_{O_2}/p_{SO_2} is locally higher than the equilibrium ratio for the reaction at the temperature under consideration. Take for example, roasting of sphalerite (ZnS):

$$2ZnS(s) + 3O_2(g) = 2ZnO(s) + 2SO_2(g) \tag{2.20}$$

$$K = \frac{p_{SO_2}^2}{p_{O_2}^3} \tag{2.21}$$

For reaction (2.20) to proceed, it is essential that at least three molecules of oxygen should reach the interface to form two molecules of sulfur dioxide, that is, $J_{O_2} \not< 3/2 J_{SO_2}$. These two flux values $(J_{O_2} \text{and} J_{SO_2})$ are controlled by the respective diffusion coefficients and partial pressure of O_2 and SO_2. The diffusion coefficient of O_2 is larger than SO_2 molecules but there is always a minimum ratio of p_{O_2}/p_{SO_2} in the atmosphere outside the particle. This minimum ratio has to be maintained so as to keep the ratio at the reaction front always higher than the equilibrium value.

As usual the reaction mechanism may occur in several stages:

1. Adsorption of oxygen at the surface of the sulfide mineral particles.
2. Incorporation of oxygen in the lattice of the mineral after release of electrons $\left(\frac{1}{2}O_2 = O^{2-} + 2e\right)$ and neutralization of sulfide ion on the surface by the electrons ($S^{2-} + 2e = S$).
3. Chemical reaction between the adsorbed sulfur atom and adsorbed oxygen atom.
4. Desorption of SO_2 molecule.
5. Migration of SO_2 leaves a vacant site on the mineral surface.

Another sulfide ion may move to occupy this site to continue the reaction further but generally the interface [2] advances into the mineral to reach more sulfide ions. However, the role of adsorption is not very clear. It may be helpful in reducing the activation energy and increasing the rate of roasting reactions. The reaction rate is controlled by the number of oxygen molecules adsorbed per unit area of interface, which is proportional to the partial pressure of oxygen as expected according to the laws of adsorption. The larger the particle, the higher will be the p_{O_2} required to maintain a particular flux (J_{O_2}) at the reaction interface. In case of total oxidation (i.e., dead roasting) attempt should be made to increase p_{O_2} in the gaseous mixture around the mineral particles in the last stages.

The following points must be kept in mind while carrying out roasting:

1. In case of nonuniform temperature throughout the ore lump, diffusion should be considered as going down a "chemical potential gradient" rather than a partial pressure gradient.
2. As ore particles are not homogeneous lumps of sulfide, the presence of inert gangue may reduce or even stop reactions.

3. Exothermicity of roasting reactions may lead to fusion or agglomeration of particles, thereby altering the diffusion coefficients and diffusion paths and thus, ultimately, slowing down the process.
4. Depending on operating conditions, side reactions, for example, sulfate formation may occur in the cooler part of the outer oxide shell.

By and large, roasting of zinc sulfide is carried out at and above 800°C to produce zinc oxide. This is known as dead roasting. The rate of oxidation is very slow at 700°C. At lower temperatures [16] ZnS reacts with SO_3 to form $ZnSO_4$ according to the reactions:

$$ZnS(s) + 4SO_3(g) \rightarrow ZnSO_4(s) + 4SO_2(g) \tag{2.22}$$

$$ZnS(s) + O_2(g) + 2SO_3(g) \rightarrow ZnSO_4(s) + 2SO_2(g) \tag{2.23}$$

In the absence of SO_3 sulfation does not take place when ZnS is treated with SO_2 and air. Sulfates are generally stable at temperatures below 800°C at a lower p_{O_2}/p_{SO_2} ratio. Hence, sulfation of fine concentrate is restricted in a separate part of the kiln by maintaining a lower temperature and higher SO_2 in the gaseous mixture.

A bulk of fine concentrate behaves like a single large lump against the reacting gases. In such cases the solid–gas contact area is increased by raking or fluidization in order to improve the rate of roasting because gases normally penetrate the solid particles through inter-granular routes rather than though the crystals. As the individual crystal gets converted topochemically to the product, the radial rate of conversion is the same all the way around. The rate of reaction decreases toward the centre of the ore particle. Hence, the rate of reaction on the inner grains (deeper into the particles) will be determined by an entirely different mechanism from the particle as a whole. It is most likely that a solid state diffusion mechanism may be operative within the grains. In the case of coarse grains this mechanism can take control of the reaction rate for the particle as a whole.

Natesan and Philbrook [17, 18] studied the kinetics of roasting of zinc sulfide spherical pellets [17] and powder under suspension [18] in a fluidized bed reactor. In the temperature range of 740–1040°C, roasting of pellets of 0.1.6 cm diameter according to the reaction (2.20) is controlled by gaseous transport through the product layer of zinc oxide formed during the course of the reaction. On the other hand, in the fluidized bed reactor for the suspended particles the kinetics is governed by the surface reaction at the ZnS—ZnO interface in the same temperature range.

Based on their detailed studies on roasting of covellite (CuS) in oxygen, Shah and Khalafallah [19] have proposed the following sequence of conversion:

$$CuS \rightarrow Cu_{1.8}S \rightarrow Cu_2O \rightarrow CuO \rightarrow CuO{\cdot}CuSO_4 \rightarrow CuSO_4 \tag{2.24}$$

$Cu_{1.8}S$ is considered to be a defective form of copper sulfide, known as digenite. After establishing the sequence of roasting the kinetics of the first [20, 21] and last steps [22] in Equation 2.24 was systematically investigated. The conversion of covellite (CuS) to digenite ($Cu_{1.8}S$) was studied in nitrogen [20] and oxygen [21] atmosphere for the reactions:

$$\text{In nitrogen}\,(340-400^\circ\text{C}): 1.8\text{CuS(s)} \rightarrow \text{Cu}_{1.8}\text{S(s)} + 0.4\,\text{S}_2\text{(g)} \qquad (2.25)$$

$$\text{In oxygen}\,(260-400^\circ\text{C}): 1.8\text{CuS(s)} + 0.8\text{O}_2\text{(g)} \rightarrow \text{Cu}_{1.8}\text{S(s)} + 0.8\text{SO}_2\text{(g)} \qquad (2.26)$$

In nitrogen, the reaction was found to be topochemical with the activation energy of 24 ± 2 kcal mol^{-1}. The rate of conversion in oxygen was first order with respect to the partial pressure of oxygen with an average apparent activation energy of 23 ± 3 kcal mol^{-1}.

Rao and Abraham [7] have reported two stages in the kinetics of roasting of cuprous sulfide in the temperature range of 750–950°C. The kinetics of the initial non-isothermal stage with an activation energy of 25 kcal mol^{-1} is controlled by heat and mass transport whereas the second isothermal stage with an apparent activation energy of about 6 kcal mol^{-1} is controlled by mass transport. The mass transport involves diffusion through an outer boundary layer, diffusion through the layer formed during a nonisothermal period, and diffusion through a product layer formed during a continuing reaction.

Coudurier et al. [23] conducted studies on roasting of molybdenite (MoS_2) in an experimental multiple hearth roaster and reported that the rate of reaction was controlled by gaseous diffusion on the upper hearth and by surface reaction on the lower hearth. Different equations developed for the upper and lower hearths were useful in deriving optimum operating conditions by matching the heat balance with the reaction kinetics. In conclusion, they have proposed that the kinetics of roasting of molybdenite was controlled by gaseous diffusion in the early stages and by surface reaction in the later stages of the reaction. Amman and Loose [24] investigated the effects of temperature (525–635°C), gas composition (5–20% oxygen), and particle size on the oxidation kinetics of molybdenite concentrate containing 90% MoS_2. They proposed a mathematical model to explain the reaction kinetics involving diffusion of oxygen from the bulk gas phase to the solid interface, diffusion through reaction product layer, and a first order reaction kinetics at the molybdenite–oxide interface with an activation energy of 35.4 kcal mol^{-1}. This order of activation energy simply indicates that the oxidation kinetics of molybdenite in the temperature range of 525–635°C, is chemically controlled.

In the temperature range of 690–800°C, lead sulfide is converted to lead sulfate according to the reaction:

$$\text{PbS(s)} + 2\text{O}_2\text{(g)} = \text{PbSO}_4\text{(s)} \qquad (2.27)$$

The sulfation roasting of galena follows the kinetic law [25]:

$$1 + 2(1 - z{\cdot}f) - 3(1 - z{\cdot}f)^{2/3} = \frac{k}{4r_0^2}\,t \qquad (2.28)$$

In Equation 2.28, f is fraction of PbS converted into $PbSO_4$ and z the volume of $PbSO_4$ formed per unit volume of PbS and k, r_0 and t represent respectively, the rate constant, initial radius of the sulfide particle, and time of reaction. From the diffusion measurement experiments it has been established that PbS diffuses from the inside through the $PbSO_4$ layer to react on the surface. The kinetics of roasting of galena expressed by the rate Equation 2.28 is very much similar to the well-known Ginstling-Brounshtein [26] product layer diffusion equation, which will be discussed in Chapter 5. The roasting according to Equation 2.27 is sensitive to particle size.

2.6 PREDOMINANCE AREA DIAGRAMS AS A USEFUL GUIDE IN FEED PREPARATION

In the preceding paragraphs it has been mentioned that roasting is one of the main steps in the extraction of nickel, zinc, and molybdenum from pentlandite, sphalerite and molydenite concentrates, respectively. Recently developed faster smelting and converting processes for the production of copper from chalcopyrite concentrate do not require roasting. In this section, an attempt has been made to demonstrate as to how the predominance area diagrams of Cu—S—O and Fe—S—O systems were used in the past for the preparation of feed for reverberatory smelting and leaching circuit (though currently not practiced) by roasting of chalcopyrite at different temperatures.

The composition of roaster products prepared for reverberatory smelting was not critical but it was desirable to avoid excessive oxidation of iron. The formation of Fe_3O_4 or Fe_2O_3 led to high oxidizing conditions in the subsequent smelting slags and these oxidizing conditions caused an increased loss of copper in the slag. The formation of high melting ferrites was also favored by over oxidation of the iron minerals. Figure 2.3 that exhibits the predominance area diagram of the Fe—S—O system at different temperatures directs that the best way to avoid over oxidation, that is, Fe_2O_3 formation, was to roast at relatively low temperatures. This is demonstrated by the position of the roaster gas composition partial pressures square within the $Fe_2(SO_4)_3$ region at temperatures below about 600°C. The stable phases in Cu—S—O and Fe—S—O systems based on the diagrams have been listed in Table 2.1.

The principal objectives of roasting prior to leaching were (a) to produce a controlled amount of $CuSO_4$ with the remainder of Cu being in oxide form (b) to produce iron oxides rather than soluble iron sulfates. The latter objective minimized contaminations of the leach liquor with iron. Figure 2.4 shows that $CuSO_4$ formation is favored below 677°C, $CuSO_4$ and CuO are favored between 677 and 800°C, and CuO is favored above 800°C. Therefore, roasting to produce a mixed $CuSO_4$/CuO product should be carried out between 677 and 800°C. The higher temperature favors higher proportion of CuO. Figure 2.3 also indicates that temperature in this range also favors the formation of insoluble iron oxides, which is the second requirement. Thus, roasting at a temperature of 675°C fulfilled both the objectives.

The predominance area diagram of the Zn—S—O system [13] (Fig. 2.5) at different temperatures is useful in the preparation of feeds for Imperial smelting and leaching by roasting sphalerite concentrates at appropriate temperatures. Since the blast furnace

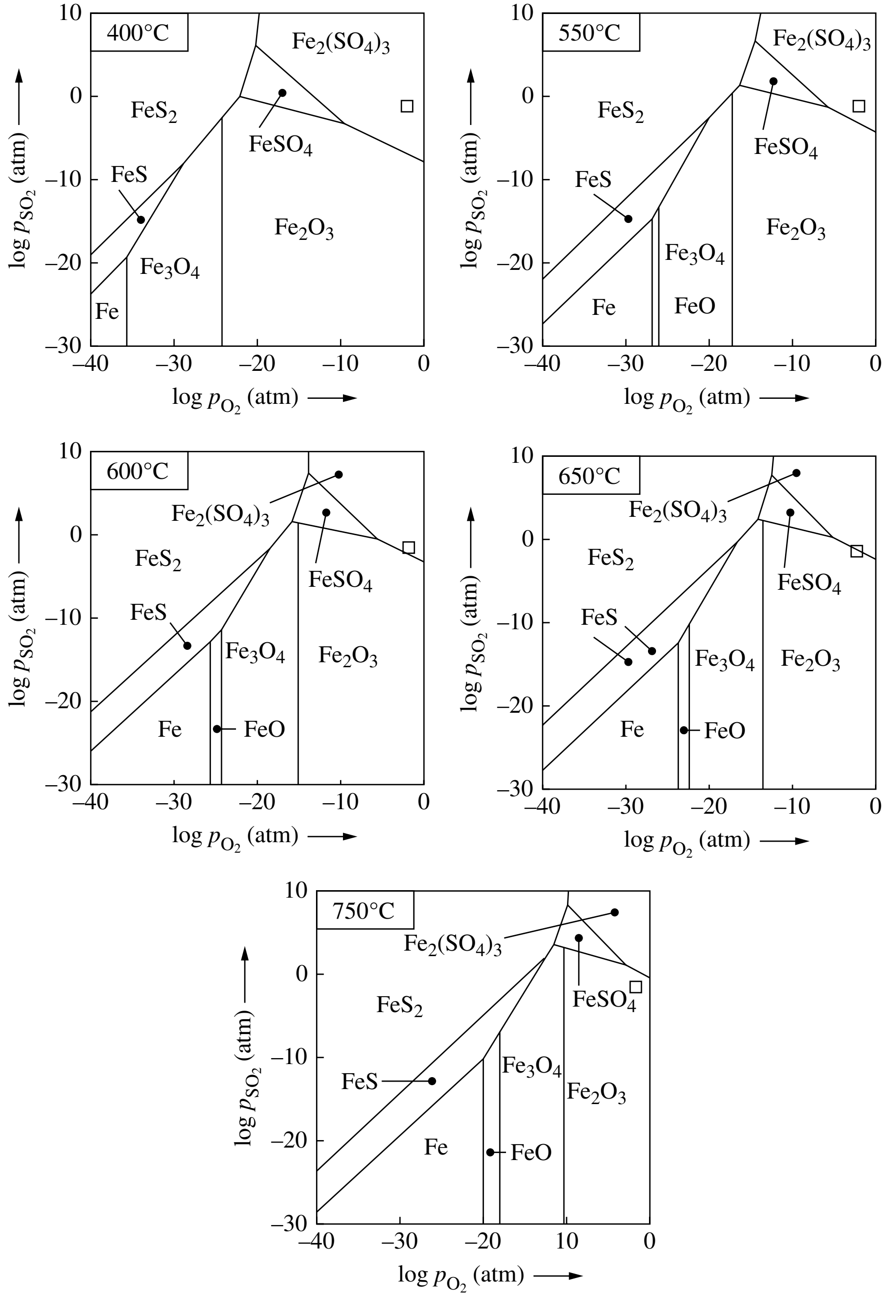

FIGURE 2.3 Predominance area diagrams of the Fe—S—O system at 400, 550, 600, 650 and 750°C. □ Usual roaster gas composition (Reproduced from M. Shamsuddin et al. [13] with the permission of Meshap Science Publishers).

TABLE 2.1 Stable Phases Expected from Cu—S—O and Fe—S—O Diagrams at Different Temperatures at Usual Roaster Gas Composition[a]

Temperature (°C)	Phases of		Remarks
	Cu	Fe	
400	$CuSO_4$	$Fe_2(SO_4)_3$	The gases leaving industrial roasters have compositions [15] in the range of 5–15% SO_2 and 1–5% O_2 (+10% H_2O and 75% N_2) which are equal to $p_{SO_2} = 10^{-1.5}$ to $10^{-0.5}$ and $p_{O_2} = 10^{-2}$ to 10^{-1} atm.
550	$CuSO_4$	$Fe_2(SO_4)_3$	
600	$CuSO_4$	$Fe_2(SO_4)_3$, Fe_2O_3	
650	$CuSO_4$	Fe_2O_3	
750	$CuO{\cdot}CuSO_4$	Fe_2O_3	

[a] Reproduced from M. Shamsuddin et al. [13] with the permission of Meshap Science Publishers.

requires more lumpy charge (size varying from 2.5 to 10 cm) the Dwight-Lloyd sintering machine is preferred over roasters for the extraction of zinc and lead. However, sphalerite concentrate is first partially roasted at 800°C to obtain a product with 4% sulfur. The resultant mass is then sintered at 1200°C to produce lumpy zinc oxide sinter for the Imperial smelting furnace. The predominance area diagrams of Zn—S—O (Fig. 2.5) and Pb—S—O (Fig. 2.6) systems indicate that the stability regions of both $ZnSO_4$ and $PbSO_4$ shrink with increase of temperature. Hence, the product that results after roasting/sintering of sphalerite and galena concentrates at 800°C will consist of mixed oxide (larger amount) and little sulfate (respectively, $ZnO + ZnSO_4$ and $PbO + PbSO_4$). From the Mo—S—O diagram (Fig. 2.8) it is clear that MoS_2 will get converted to MoO_3 while roasting molybdenite at 700°C. Therefore, in order to prevent melting due to local overheating and high volatility of MoO_3, the temperature is never allowed to exceed beyond 650°C.

2.7 PROBLEMS [27–29]

Problem 2.1

a. From the data given below construct relevant portion of the predominance area diagram of Ni—S—O system:

$$NiS(s) + \frac{3}{2}O_2(g) = NiO(s) + SO_2(g), \qquad \log K_1 = 18.87$$

$$NiS(s) + 2O_2(g) = NiSO_4(s), \qquad \log K_2 = 21.59$$

$$NiO(s) + \frac{1}{2}O_2(g) + SO_2(g) = NiSO_4(s), \qquad \log K_3 = 2.72$$

b. If nickel sulfide is roasted in a roaster gas containing SO_2 and O_2 in the composition range 2–10% SO_2 and 2–10% O_2 over what portion of these composition ranges is nickel sulfate the stable phase?

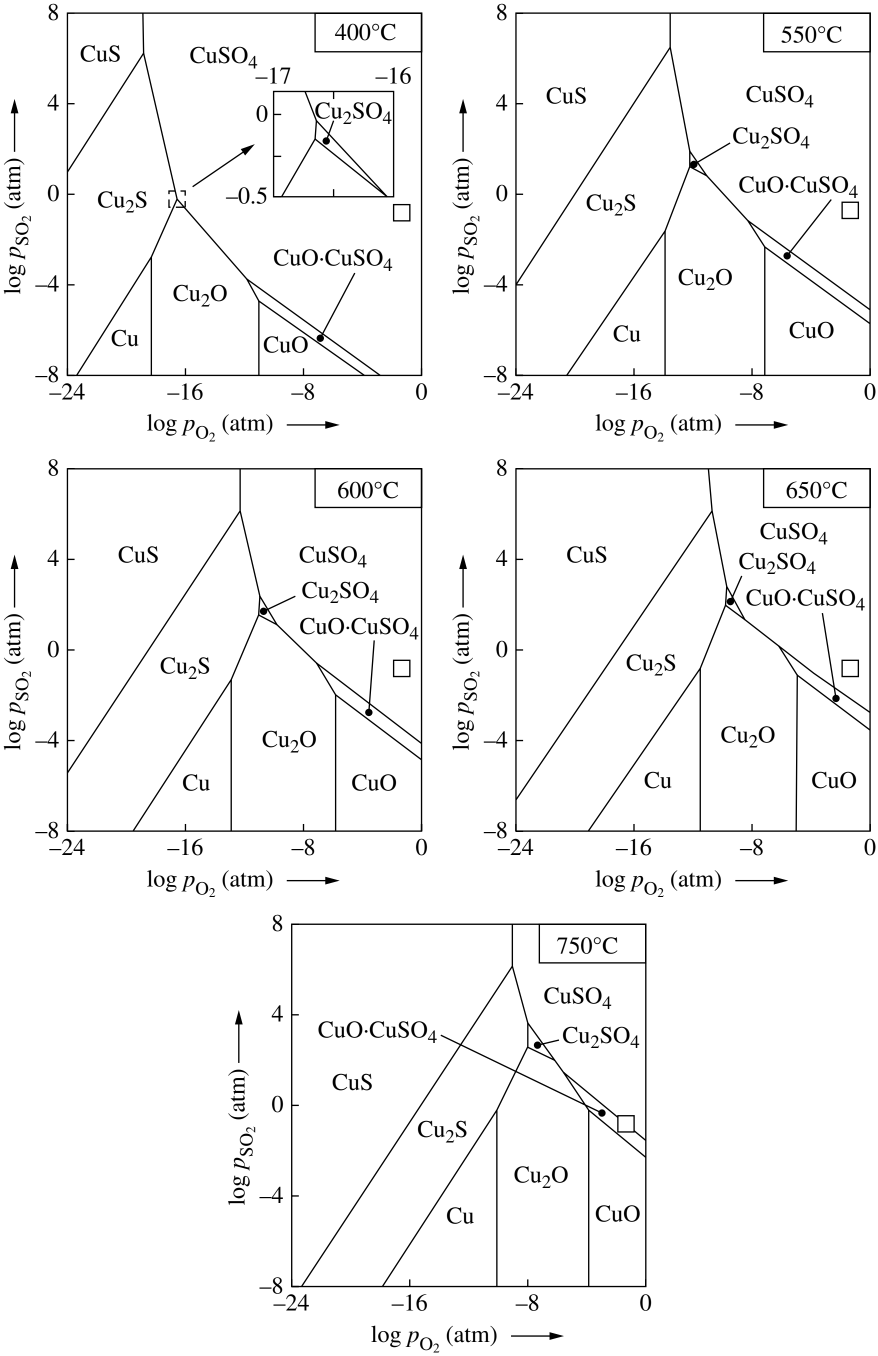

FIGURE 2.4 Predominance area diagrams of the Cu—S—O system at 400, 550, 600, 650 and 750°C. □ Usual roaster gas composition (Reproduced from M. Shamsuddin et al. [13] with the permission of Meshap Science Publishers).

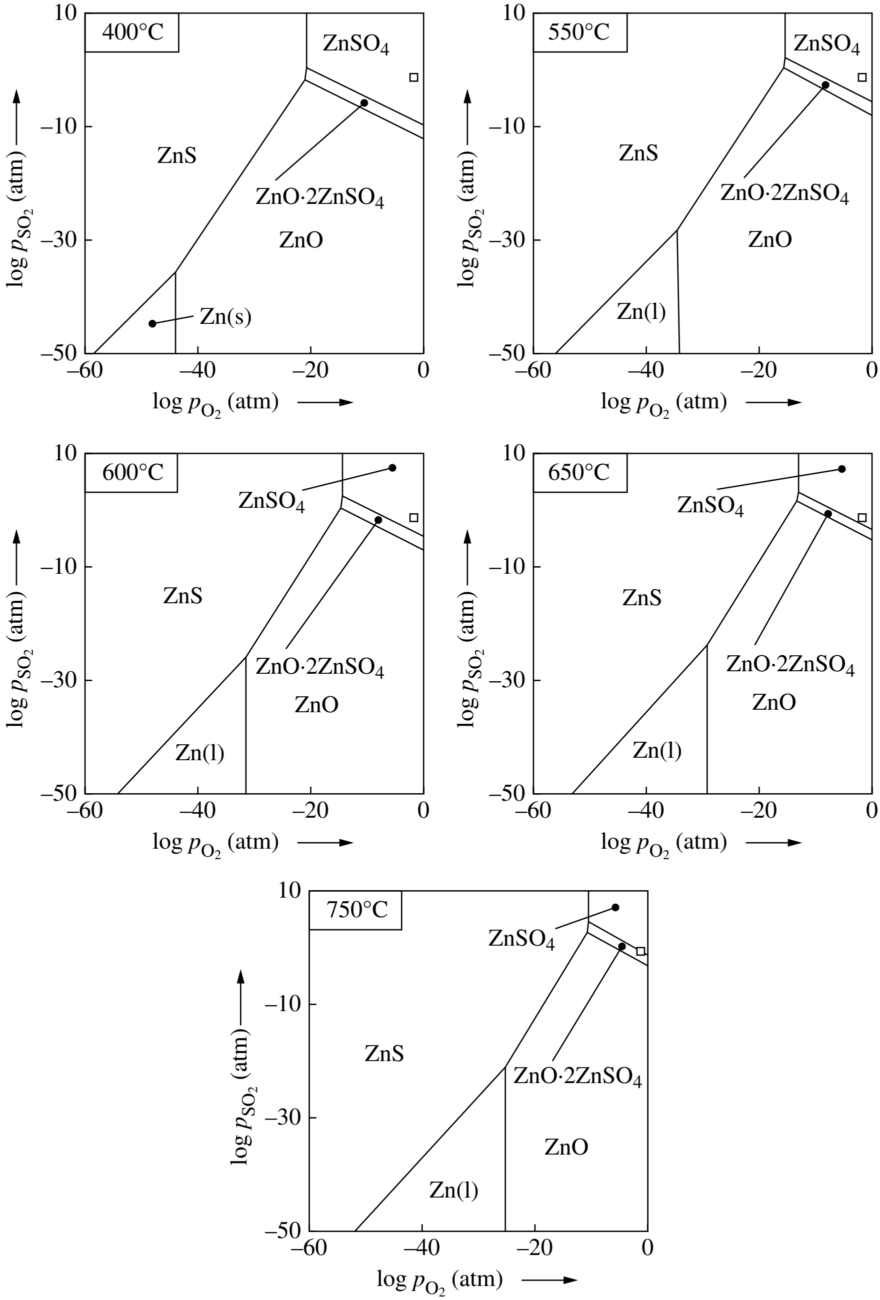

FIGURE 2.5 Predominance area diagrams of the Zn—S—O system at 400, 550, 600, 650 and 750°C. □ Usual roaster gas composition (Reproduced from M. Shamsuddin et al. [13] with the permission of Meshap Science Publishers).

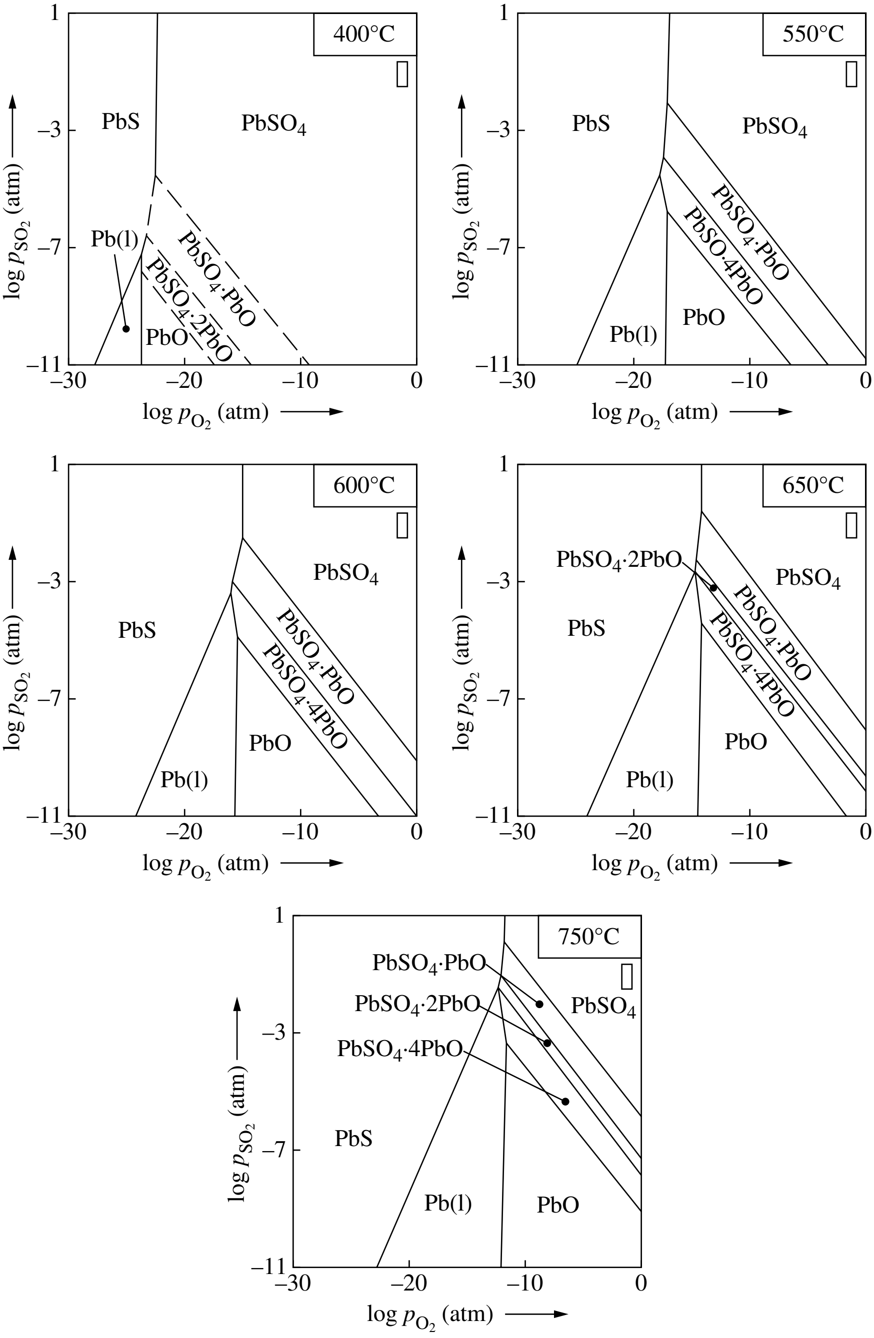

FIGURE 2.6 Predominance area diagrams of the Pb—S—O system at 400, 550, 600, 650 and 750°C. ☐ Usual roaster gas composition (Reproduced from M. Shamsuddin et al. [13] with the permission of Meshap Science Publishers).

Solution

a. From the above chemical equations:

i. For the NiS—NiO equilibrium,

$$K_1 = \frac{p_{SO_2}}{p_{O_2}^{3/2}}$$

$$\text{or } \frac{3}{2}\log p_{O_2} = \log p_{SO_2} - \log K_1$$

$$\text{or } \log p_{O_2} = \frac{2}{3}\log p_{SO_2} - \frac{2}{3}\log K_1$$

$$\therefore \log p_{O_2} = \frac{2}{3}\log p_{SO_2} - \frac{2}{3}18.87 = \frac{2}{3}\log p_{SO_2} - 12.58$$

ii. For the NiS—$NiSO_4$ equilibrium,

$$K_2 = \frac{1}{p_{O_2}^2}$$

$$2\log p_{O_2} = -\log K_2$$

$$\therefore \log p_{O_2} = -0.5\log K_2 = -0.5 \times 21.59 = -10.795$$

iii. For the NiO—$NiSO_4$ equilibrium,

$$K_3 = \frac{1}{p_{O_2}^{1/2} \cdot p_{SO_2}}$$

$$\frac{1}{2}\log p_{O_2} + \log p_{SO_2} = -\log K_3$$

$$\text{or } \log p_{O_2} = -2\log K_3 - 2\log p_{SO_2}$$

$$\therefore \log p_{O_2} = -2 \times 2.72 - 2\log p_{SO_2} = -5.44 - 2\log p_{SO_2}$$

Summary of the above calculations

Equilibria	log K	$\log p_{O_2}$
$NiS(s) + \frac{3}{2}O_2(g) = NiO(s) + SO_2(g)$	18.87	$2/3\log p_{SO_2} - 12.58$
$NiS(s) + 2O_2(g) = NiSO_4(s)$	21.59	−10.795
$NiO(s) + \frac{1}{2}O_2(g) + SO_2(g) = NiSO_4(s)$	2.72	$-5.44 - 2\log p_{SO_2}$

Figure 2.7 shows the predominance area diagram of the Ni—S—O system in terms of $\log p_{O_2}$ and $\log p_{SO_2}$.

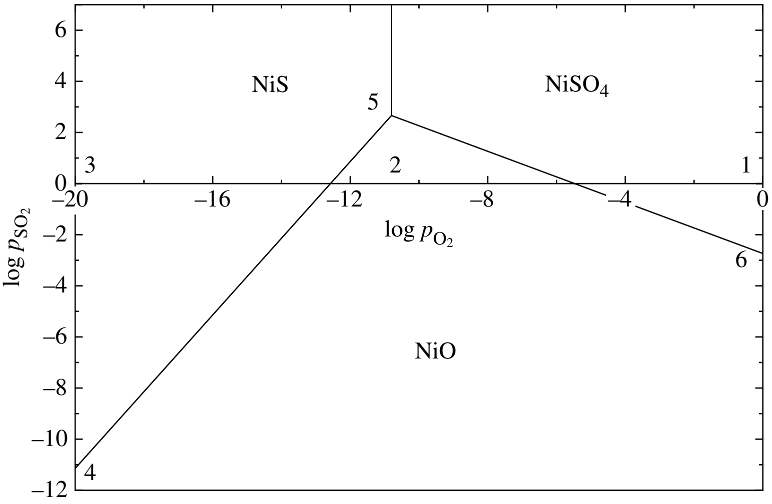

FIGURE 2.7 Relevant portion of the predominance area diagram of the Ni—S—O system.

Point 1: when $p_{O_2} = 1\,\text{atm}$, $\log p_{O_2} = 0$

A horizontal line is drawn up to $\log p_{O_2} = -20$

Vertical lines are drawn at $\log p_{O_2} = 0$ and $\log p_{O_2} = -20$

Point 2: at $\log p_{O_2} = -10.795$, a vertical line is drawn

Point 3: $\log p_{O_2} = -20$

Point 4: NiS—NiO equilibrium

$$\log p_{SO_2} = \frac{3}{2}\log p_{O_2} + \log K_1 \text{ at point 3, } \log p_{O_2} = -20$$

$$= \frac{3}{2}(-20) + 18.87 = -11.13\,(\text{point 4})$$

Point 5: NiS—NiO equilibrium, at point 2, $\log p_{O_2} = -10.795$

$$\log p_{SO_2} = \frac{3}{2}\log p_{O_2} + 18.87$$

$$= \frac{3}{2}(-10.795) + 18.87 = 2.67 \text{ (point5)}$$

Point 6: NiO—NiSO$_4$ equilibrium, at point 1, $\log p_{O_2} = 0$

$$\log p_{SO_2} = -\log K_3 - 0.5\log p_{O_2} = -2.72 \text{ (point6)}.$$

b. From the Figure 2.7 we find that NiSO$_4$ is a stable phase in the region: from $\log p_{O_2} = 0$, that is, $p_{O_2} = 1$ atm (point 1) to $\log p_{O_2} = -10.795$, that is,

$p_{O_2} = 1.6 \times 10^{-11}$ atm (point 2) and from $\log p_{SO_2} = -2.72$, that is, $p_{SO_2} =$ 0.002 atm (point 6) or $SO_2 = 0.2\%$ to $\log p_{SO_2} = 2.67$, that is, $p_{SO_2} = 467$ atm (point 5). This can be demonstrated by independent calculations also.

From the above calculations, we note that for NiS—NiO equilibrium:

$$\log K_1 = \log p_{SO_2} - \frac{3}{2}\log p_{O_2} = 18.87 \tag{1}$$

and for the NiO—$NiSO_4$ equilibrium:

$$\log K_3 = -\log p_{SO_2} - \frac{1}{2}\log p_{O_2} = 2.72 \tag{2}$$

From Equations 1 and 2 we get: $\log p_{O_2} = -10.795$, that is, $p_{O_2} = 1.6 \times 10^{-11}$ atm, and $\log p_{SO_2} = 2.67$, that is, $p_{SO_2} = 467$ atm.

Thus, $NiSO_4$ is stable from $p_{O_2} = 1.6 \times 10^{-11}$ to 1 atm ($\log p_{SO_2} = 0$ where $\log p_{SO_2} = -2.72$, that is, $p_{SO_2} = 0.002$ atm or $SO_2 = 0.2\%$), and $p_{SO_2} = 0.002$ to 467 atm Ans.

Problem 2.2

From the data given below, construct relevant portion of the predominance area diagram of the Mo—S—O system at 1000 K:

1.	$2SO_2(g) = S_2(g) + 2O_2(g)$,	$\Delta G_1^\circ = 173{,}240 - 34.62T$ cal
2.	$MoS_2(s) = Mo(s) + S_2(g)$,	$\Delta G_2^\circ = 85{,}870 - 37.33T$ cal
3.	$MoO_2(s) = Mo(s) + O_2(g)$,	$\Delta G_3^\circ = 140{,}500 + 4.6T\log T - 56.8T$ cal
4.	$MoO_3(s) = MoO_2(s) + \frac{1}{2}O_2(g)$,	$\Delta G_4^\circ = 38{,}700 - 19.5T$ cal

Solution

The following equilibria between compounds of Mo have to be considered: Mo—MoO_2, MoO_2—MoO_3, Mo—MoS_2, MoS_2—MoO_2 and MoS_2—MoO_3. ΔG° vs T equations for these equilibria may be obtained by making use of the given 4 ΔG° vs T equations.

a. $Mo(s) + O_2(g) = MoO_2(s)$, $\Delta G_a^\circ = -\Delta G_3^\circ = -140{,}500 - 4.6T\log T + 56.8T$ cal

b. $MoO_2(s) + \frac{1}{2}O_2(g) = MoO_3(s)$, $\Delta G_b^\circ = -\Delta G_4^\circ = -38{,}700 + 19.5T$ cal

c. $Mo(s) + 2SO_2(g) = MoS_2(s) + 2O_2(g)$, $\Delta G_c^\circ = \Delta G_1^\circ - \Delta G_2^\circ = 87{,}370 + 2.71T$

d. $MoS_2(s) + 3O_2(g) = MoO_2(s) + 2SO_2(g)$, $\Delta G_d^\circ = \Delta G_2^\circ - \Delta G_1^\circ - \Delta G_3^\circ$
$= -227{,}870 - 4.6T\log T + 54.09T$

e. $MoS_2(s) + \frac{7}{2}O_2(g) = MoO_2(s) + 2SO_2(g)$, $\Delta G_e^\circ = \Delta G_2^\circ - \Delta G_1^\circ - \Delta G_3^\circ - \Delta G_4^\circ$
$= -266{,}570 - 4.6T\log T + 73.59T$

From the above ΔG vs T equations calculated, values of ΔG°_{1000}, $\log K$ and $\log p_{O_2}$ for different equilibria are summarized below:

Equilibria	ΔG°_{1000}	$\log K$	$\log p_{O_2}$
$Mo(s) + O_2(g) = MoO_2(s)$	−97,500	21.3	−21.3
$MoO_2(s) + \frac{1}{2}O_2(g) = MoO_3(s)$	−19,200	4.2	−8.4
$Mo(s) + 2SO_2(g) = MoS_2(s) + 2O_2(g)$	+90,080	−19.7	$\log p_{SO_2} - 9.85$
$MoS_2(s) + 3O_2(g) = MoO_2(s) + 2SO_2(g)$	−187,580	41.0	$2/3 \log p_{SO_2} - 13.66$
$MoS_2(s) + \frac{7}{2}O_2(g) = MoO_3(s) + 2SO_2(g)$	−206,780	45.2	$2/3.5 \log p_{SO_2} - 12.91$

a. $Mo—MoO_2$ equilibrium,

$$K_a = \frac{1}{p_{O_2}}$$

$$\therefore \log p_{O_2} = -\log K_a = -21.3$$

b. $MoO_2—MoO_3$ equilibrium,

$$K_b = \frac{1}{p_{O_2}^{1/2}}$$

$$\therefore \log p_{O_2} = -2 \log \log K_b = -2 \times 4.2 = -8.4$$

c. $MO—MoS_2$ equilibrium,

$$K_c = \frac{p_{O_2}^2}{p_{SO_2}^2}$$

$$\therefore \log p_{O_2} = \frac{1}{2}\log K_c + \log p_{SO_2} = -\frac{1}{2} \times 19.7 + \log p_{SO_2} = -9.85 + \log p_{SO_2}$$

d. $MoS_2—MoO_2$ equilibrium,

$$K_d = \frac{p_{SO_2}^2}{p_{O_2}^3}$$

$$\therefore \log p_{O_2} = -\frac{1}{3}\log K_d + \frac{2}{3}\log p_{SO_2} = -\frac{41.0}{3} + \frac{2}{3}\log p_{SO_2} = -13.66 + \frac{2}{3}\log p_{SO_2}$$

e. MoS_2—MoO_3 equilibrium,

$$K_e = \frac{p_{SO_2}^2}{p_{O_2}^{3.5}}$$

$$\therefore \log p_{O_2} = -\frac{1}{3.5}\log K_e + \frac{2}{3.5}\log p_{SO_2} = -\frac{1}{3.5}\times 45.2 + \frac{2}{3.5}\log p_{SO_2}$$
$$= -12.91 + \frac{2}{3.5}\log p_{SO_2}$$

Construction of the diagram:

I. Draw a vertical line at $\log p_{O_2} = 0$ i.e. $p_{O_2} = 1$ atm (Y-axis) and a horizontal line at $\log p_{SO_2} = 0$, that is, $p_{SO_2} = 1$ atm (X-axis)
Draw vertical lines at $\log p_{O_2} = -8.4$ and -21.3, respectively, demonstrating the MoO_2—MoO_3 and Mo—MoO_2 equilibria. Mark $\log p_{O_2} = 0$ and -40 on X-axis and $\log p_{SO_2} = \pm 25$ on Y-axis.
Thus, at $\log p_{SO_2} = -25$, we have point 1, $\log p_{O_2} = -21.3$, point 2, $\log p_{O_2} = -8.4$ and point 3, $\log p_{O_2} = 0$.

II. At point 4 on the vertical line exhibiting the Mo—MoO_2 equilibrium, consider the Mo—MoS_2 equilibrium $(\log p_{O_2} = -21.3)$

$$\log p_{O_2} = -9.85 + \log p_{SO_2}$$
$$\text{or } \log p_{SO_2} = \log p_{O_2} + 9.85 = -21.3 + 9.85 = -11.45$$

III. At point 5 on the vertical line exhibiting the MoO_2—MoO_3 equilibrium, consider the MoO_2—MoS_2 equilibrium $(\log p_{O_2} = -8.4)$

$$\log p_{O_2} = -13.66 + \frac{2}{3}\log p_{SO_2}$$
$$\text{or } \frac{2}{3}\log p_{SO_2} = \log p_{O_2} + 13.66 = -8.4 + 13.66 = 5.26$$
$$\text{or } \log p_{SO_2} = 3/2 \times 5.3 = 7.95$$

IV. At point 6 on the vertical line exhibiting the MoO_3—O_2 equilibrium, consider the MoS_2—MoO_3 equilibrium $(\log p_{O_2} = 0)$

$$\log p_{O_2} = -12.91 + 2/3.5 \log p_{SO_2} = 0$$
$$\text{or } \log p_{SO_2} = 22.6$$

V. At point 7, $\log p_{SO_2} = -25$ and $\log p_{O_2} = 0$

VI. At point 8, $\log p_{SO_2} = -25$, consider Mo—MoS_2 equilibrium,

$$\log p_{O_2} = -9.85 + \log p_{SO_2} = -9.85 - 25 = -34.85 \sim -34.9$$

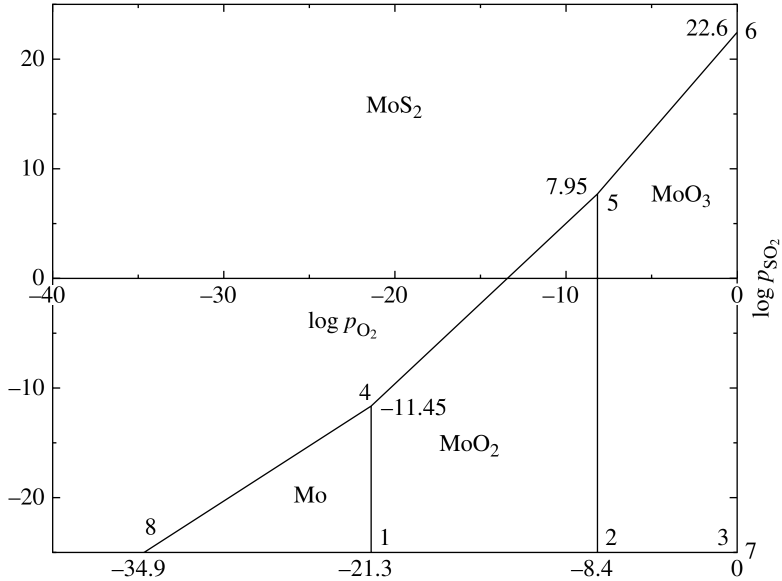

FIGURE 2.8 Relevant portion of the predominant area diagram of the Mo—S—O system.

Figure 2.8 shows the predominance area diagram of the Mo—S—O system at 1000 K.

Problem 2.3

Given the following data construct the predominance area diagram for copper compounds in the presence of oxygen and sulfur dioxide at 900 K.

Reactions	ΔG° (cal)
$2Cu(s) + \frac{1}{2}O_2(g) = Cu_2O(s)$	$-40{,}500 - 3.92T \log T + 29.5T$
$Cu_2O(s) + \frac{1}{2}O_2(g) = 2CuO(s)$	$-34{,}950 - 6.10T \log T + 44.3T$
$2Cu(s) + \frac{1}{2}S_2(g) = Cu_2S(s)$	$-34{,}150 - 6.20T \log T + 28.7T$
$2Cu_2S(s) + S_2(g) = 4CuS(s)$	$-45{,}200 + 54.0T$
$S_2(g) + 2O_2(g) = 2SO_2(g)$	$-173{,}240 + 34.6T$
$SO_2(g) + \frac{1}{2}O_2(g) = SO_3(g)$	$-22{,}600 + 21.36T$
$Cu(s) + 2O_2(g) + \frac{1}{2}S_2(g) = CuSO_4(s)$	$-183{,}000 + 88.4T$
$SO_3(g) + 2CuO(s) = CuO{\cdot}CuSO_4(s)$	$-49{,}910 - 3.32T \log T + 50.1\,T$
$Cu_2O(s) + SO_3(g) = Cu_2SO_4(s)$	$-44{,}800 + 39.9T$

Solution

Based on the above ΔG° vs T equations given in the problem, ΔG°_{900} and log K_{900} for various reactions related to different compounds in the Cu—S—O system were calculated. The relationship between p_{O_2} and p_{SO_2} for various reactions, which determine the predominant areas are listed below:

Reaction		ΔG°_{900} kcal	log K_{900}	$\log p_{O_2} = f(\log p_{SO_2})$
1.	$2Cu + \frac{1}{2}O_2 = Cu_2O$	−24.37	5.92	$\log p_{O_2} = -11.84$
2.	$Cu_2O + \frac{1}{2}O_2 = 2CuO$	−11.30	2.74	$\log p_{O_2} = -5.48$
3.	$2CuS + O_2 = Cu_2S + SO_2$	−72.75	17.66	$\log p_{O_2} = -17.66 + \log p_{SO_2}$
4.	$Cu_2S + O_2 = 2Cu + SO_2$	−46.16	11.21	$\log p_{O_2} = -11.21 + \log p_{SO_2}$
5.	$Cu_2S + \frac{3}{2}O_2 = Cu_2O + SO_2$	−70.62	17.15	$\log p_{O_2} = -11.43 + 2/3 \log p_{SO_2}$
6.	$CuS + 2O_2 = CuSO_4$	−91.89	22.31	$\log p_{O_2} = -11.16$
7.	$Cu_2S + 3O_2 + SO_2 = 2CuSO_4$	−111.03	26.96	$\log p_{O_2} = -8.99 - 1/3 \log p_{SO_2}$
8.	$Cu_2O + \frac{3}{2}O_2 + 2SO_2 = 2CuSO_4$	−40.41	9.81	$\log p_{O_2} = -6.54 - 4/3 \log p_{SO_2}$
9.	$CuO{\cdot}CuSO_4 + SO_2 + \frac{1}{2}O_2 = 2CuSO_4$	−12.09	2.93	$\log p_{O_2} = -5.87 - 2 \log p_{SO_2}$
10.	$Cu_2O + SO_2 + O_2 = CuO{\cdot}CuSO_4$	−28.32	6.88	$\log p_{O_2} = -6.88 - \log p_{SO_2}$
11.	$2CuO + SO_2 + \frac{1}{2}O_2 = CuO{\cdot}CuSO_4$	−17.02	4.13	$\log p_{O_2} = -8.26 - 2 \log p_{SO_2}$
12.	$Cu_2S + 2O_2 = CuSO_4$	−82.88	20.13	$\log p_{O_2} = -10.07$
13.	$Cu_2O + SO_2 + \frac{1}{2}O_2 = CuSO_4$	−12.27	2.98	$\log p_{O_2} = -5.96 - 2 \log p_{SO_2}$
14.	$Cu_2SO_4 + SO_2 + O_2 = 2CuSO_4$	−28.14	6.83	$\log p_{O_2} = -6.83 - \log p_{SO_2}$
15.	$Cu_2SO_4 + \frac{1}{2}O_2 = CuO{\cdot}CuSO_4$	−16.06	3.93	$\log p_{O_2} = -7.80$

Based on the above table and following the procedure outlined in Problems 2.1 and 2.2 the predominance area diagram of the Cu—S—O system constructed is shown in Figure 2.9.

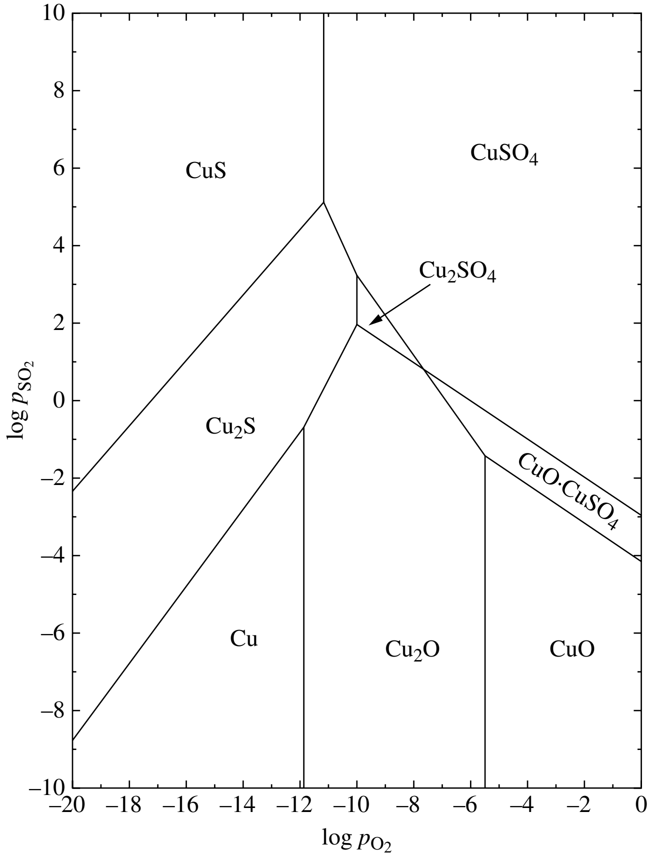

FIGURE 2.9 Predominance area diagram of the Cu—S—O system.

Problem 2.4

Galena is roasted at 750°C and 1 atm pressure in a roaster gas containing 10% SO_2 and 5% O_2. (a) Do you think $PbSO_4$ is a stable phase at this temperature in the roaster? (b) Calculate the partial pressure of SO_2 required to form $PbSO_4$ at 750°C, if the gaseous mixture contains 1% O_2. (c) What is the maximum partial pressure of SO_2 at which Pb and PbO can coexist at 750°C without forming $PbSO_4 \cdot 4PbO$?

Given that:

$$SO_2(g) + \frac{1}{2}O_2(g) = SO_3(g), \Delta G_1^\circ = -22{,}600 + 21.36T \text{ cal.} \quad (1)$$

$$2\mathrm{PbSO_4(s)} = \mathrm{PbSO_4{\cdot}PbO(s)} + \mathrm{SO_2(g)} + \frac{1}{2}\mathrm{O_2(g)} \qquad (2)$$
$$\Delta G_2^\circ = 96{,}700 + 16.81T\log T - 118.76T\,\text{cal.}$$

$$2\mathrm{PbO(s)} = 2\mathrm{Pb(l)} + \mathrm{O_2}(g), \quad \Delta G_3^\circ = 106{,}600 - 51.40T \text{ cal.} \qquad (3)$$

$$\mathrm{PbSO_4{\cdot}4PbO(s)} = 5\mathrm{PbO(s)} + \mathrm{SO_2(g)} + \frac{1}{2}\mathrm{O_2(g)}, \quad \Delta G_4^\circ = 95{,}470 - 52.10T\,\text{cal.} \qquad (4)$$

Solution

a. At 750°C (1023 K) for the reaction:

$$\mathrm{SO_2(g)} + \frac{1}{2}\mathrm{O_2(g)} = \mathrm{SO_3(g)} \qquad (1)$$

$$\Delta G_1^\circ = -22{,}600 + 21.36 \times 1023 = -748.72\,\text{cal} = -RT\ln K_1$$

$$\ln K_1 = \frac{748.72}{1.987 \times 1023} = 0.3684$$

$$\therefore\ K_1 = 1.445$$

For Equation 1, $K_1 = \dfrac{p_{\mathrm{SO_3}}}{p_{\mathrm{SO_2}} \cdot p_{\mathrm{O_2}}^{1/2}}$ $\quad p_{\mathrm{SO_2}} = 0.1\,\text{atm}\ \ p_{\mathrm{O_2}} = 0.05\,\text{atm}.$

$$p_{\mathrm{SO_3(existing)}} = K_1 \cdot p_{\mathrm{SO_2}} \cdot p_{\mathrm{O_2}}^{1/2} = 1.445 \times 0.1 \times (0.05)^{1/2} = 0.0323\,\text{atm}$$

This $p_{\mathrm{SO_3(existing)}}$ may be compared with the equilibrium $p_{\mathrm{SO_3}}$ for the reaction:

$$2\mathrm{PbSO_4(s)} = \mathrm{PbSO_4{\cdot}PbO(s)} + \mathrm{SO_3(g)} \qquad (5)$$
$$K_5 = p_{\mathrm{SO_3(equilibrium)}}$$

The standard free energy change for reaction (5) can be obtained by adding ΔG_1° and ΔG_2°

$$\therefore\ \Delta G_5^\circ = \Delta G_1^\circ + \Delta G_2^\circ = 74{,}100 + 16.8T\log T - 97.4T$$

At 1023 K, $\Delta G_5^\circ = 26{,}189\,\text{cal} = -RT\ln K_5$

$$\ln K_5 = -\frac{26{,}189}{1.987 \times 1023} = -12.884$$

$$\therefore\ K_5 = 2.54 \times 10^{-6} = p_{\mathrm{SO_3(equilibrium)}}$$

Since this equilibrium $p_{\mathrm{SO_3}} = 2.54 \times 10^{-6}$ atm is much lower than the existing equilibrium $p_{\mathrm{SO_3}} = 0.0323\,\text{atm}$ in the roaster gas, $\mathrm{PbSO_4}$ is a thermodynamically stable phase.

b. If the roasting gas containing 1% O_2 is in equilibrium with $PbSO_4$ and $PbSO_4{\cdot}PbO$, p_{SO_2} may be calculated as:

$$p_{SO_2} = \frac{p_{SO_3}}{K_1 \cdot p_{O_2}^{1/2}} = \frac{2.54 \times 10^{-6}}{1.445 \times (0.01)^{1/2}} = 1.8 \times 10^{-5}\text{atm} \quad \text{Ans.}$$

Since the partial pressure of SO_2 (=1.8×10^{-5} atm) in the roaster gas is very low, $PbSO_4$ will get converted into $PbSO_4{\cdot}PbO$ in the presence of 1% O_2.

c. At 750°C (1023 K) for the reaction: $2PbO(s) = 2Pb(l) + O_2(g)$, $K_3 = p_{O_2}$

$$\begin{aligned}\Delta G_3^\circ &= 106{,}600 - 51.40 \times 1023T = 54{,}018\,\text{cal} = -RT\ \ln p_{O_2} \\ \log p_{O_2} &= -11.5422\end{aligned} \tag{5}$$

Similarly for reaction: $PbSO_4{\cdot}4PbO(s) = 5PbO(s) + SO_2(g) + \frac{1}{2}O_2(g)$ we can express:

$$\log p_{O_2} = -18.022 - 2\log p_{SO_2} \tag{6}$$

On substituting the value of $\log p_{O_2} = -11.5422$, from Equation 5 in Equation 6, we get:

$$\log p_{SO_2} = -3.2399,$$
$$\therefore\ p_{SO_2} = 5.7 \times 10^{-4}\text{atm} \quad \text{Ans.}$$

Problem 2.5

Sphalerite is roasted at 750°C and 1 atm pressure in a roaster gas containing 10% SO_2 and 5% O_2. (a) Comment on the relative stability of $ZnSO_4$ and $ZnO{\cdot}2ZnSO_4$ phases at this temperature in the roaster. (b) Calculate the partial pressure of SO_2 required to form $ZnO{\cdot}2ZnSO_4$ at 750°C, if the gaseous mixture contains 1% O_2. (c) Calculate the maximum partial pressure of SO_2 at which three phases Zn(l), ZnS(s) and ZnO(s) will coexist at 750°C.

Given that:

$$SO_2(g) + \frac{1}{2}O_2(g) = SO_3(g), \quad \Delta G_1^\circ = -22{,}600 + 21.36T\,\text{cal}. \tag{1}$$

$$3ZnSO_4(s) = ZnO{\cdot}2ZnSO_4(s) + SO_3(g), \quad \Delta G_2^\circ = 39{,}281 - 31.87T\,\text{cal}. \tag{2}$$

$$2Zn(l) + O_2(g) = 2ZnO(s), \quad \Delta G_3^\circ = -171{,}680 - 13.80T\log T + 93.30T\,\text{cal}. \tag{3}$$

$$ZnS(s) + \frac{3}{2}O_2(g) = ZnO(s) + SO_2(g), \quad \Delta G_4^\circ = -107{,}070 - 2.30T\log T + 24.77T\,\text{cal}. \tag{4}$$

Solution

From the previous calculation in problem 2.4, for the reaction: $SO_2(g) + \frac{1}{2}O_2(g) = SO(g)$, at 1023 K, $K_1 = 1.445$ and $p_{SO_3(\text{existing})} = 3.23 \times 10^{-2}\text{atm}$

This $p_{SO_3(\text{existing})}$ may be compared with the equilibrium p_{SO_3} in the reaction:

$$3ZnSO_4(s) = ZnO{\cdot}2ZnSO_4(s) + SO_3(g) \tag{2}$$

$$\Delta G_2^{\circ} = 39{,}281 - 31.87T\text{cal.}$$

at 1023 K, $\Delta G_2^{\circ} = 39{,}281 - 31.87 \times 1023 = +7701$ cal.

$$\ln K_2 = -\frac{7701}{1.987 \times 1023} = -3.7886$$
$$\therefore K_2 = 2.3 \times 10^{-2}\text{atm} = p_{SO_3(\text{equilibrium})}$$

a. Since this equilibrium $p_{SO_3}\left(= 2.3 \times 10^{-2}\text{atm}\right)$ is very close to the existing equilibrium $p_{SO_3}\left(= 3.23 \times 10^{-2}\text{atm}\right)$ of the roaster gas, $ZnSO_4$ as well as $ZnO{\cdot}2ZnSO_4$ will coexist at 750°C in the roaster at the given gas composition.

b. If the roaster gas containing 1% O_2 is in equilibrium with $ZnSO_4$ and $ZnO{\cdot}2ZnSO_4$, p_{SO_2} may be calculated as:

$p_{SO_2} = \dfrac{p_{SO_3}}{K{\cdot}p_{O_2}^{1/2}} = \dfrac{2.3 \times 10^{-2}}{1.445 \times (0.01)^{1/2}} = 0.159\text{atm}$ (about 16% SO_2 in the gas mixture) The roaster gas containing 16% SO_2 and 1% O_2 will covert (sulfatize) ZnO into $ZnO{\cdot}2ZnSO_4$. Ans.

c. At 750°C (1023 K) for the reaction: $2Zn(l) + O_2(g) = 2ZnO(s)$, $K_3 = 1/p_{O_2}$

$$\begin{aligned} \Delta G_3^{\circ} &= -118{,}256\text{cal} = RT\ln p_{O_2} \\ \log p_{O_2} &= -25.3675 \end{aligned} \tag{5}$$

Similarly for the reaction (4): $ZnS(s) + \frac{3}{2}O_2(g) = ZnO(s) + SO_2(g)$ we can express:

$$\log p_{O_2} = -12.6507 + \frac{2}{3}\log p_{SO_2} \tag{6}$$

On substituting the value of $\log p_{O_2} = -25.3675$, from Equation 5 in Equation 6, we get:

$$\log p_{SO_2} = -19.0773,$$
$$\therefore p_{SO_2} = 8.37 \times 10^{-20}\text{atm} \quad \text{Ans.}$$

Problem 2.6

An off-grade copper concentrate contains chalcopyrite, pyrite, sphalerite, and galena. Referring to the predominance area diagrams of the systems Fe—S—O (Fig. 2.3), Cu—S—O (Fig. 2.4), Zn—S—O (Fig. 2.5) and Pb—S—O (Fig. 2.6) comment whether selective sulfation roasting of copper and zinc is possible at about 600°C. Explain by listing the stable phases at different temperatures. The usual roaster gas compositions are in the range: $p_{SO_2} = 10^{-1.5}$ to $10^{-0.5}$ and $p_{O_2} = 10^{-2}$ to 10^{-1} atm.

Solution

Since the roaster gas compositions of SO_2 (varying from $p_{SO_2} = 10^{-1.5}$ to $10^{-0.5}$ atm) and O_2 (varying from $p_{O_2} = 10^{-2}$ to 10^{-1} atm) are marked in figures, a summary of stable phases expected to form at different temperatures can be listed by referring to the predominance area diagrams of the systems: Fe—S—O (Fig. 2.3), Cu—S—O (Fig. 2.4), Zn—S—O (Fig. 2.5) and Pb—S—O (Fig. 2.6).

Stable phases expected from the M*—S—O diagrams at different temperatures and usual roaster gas compositions

Temperature (°C)	Stable Phases			
400	$CuSO_4$	$Fe_2(SO_4)_3$	$ZnSO_4$	$PbSO_4$
550	$CuSO_4$	$Fe_2(SO_4)_3$	$ZnSO_4$	$PbSO_4$
600	$CuSO_4$	$Fe_2(SO_4)_3$, Fe_2O_3	$ZnSO_4$	$PbSO_4$
650	$CuSO_4$	Fe_2O_3	$ZnSO_4$	$PbSO_4$
750	$CuO{\cdot}CuSO_4$	Fe_2O_3	$ZnO{\cdot}2ZnSO_4$	$PbSO_4$

*M stands for Fe, Cu, Zn and Pb.

On the basis of the information listed above it may be concluded that during roasting at temperatures varying from 400 to 600°C all the four metals form only their sulfates except iron that may form Fe_2O_3 at 600°C. At 750°C copper and zinc may be converted to their basic sulfates, $CuO{\cdot}CuSO_4$ and $ZnO{\cdot}2ZnSO_4$. Some of the copper may report as CuO and $CuSO_4$ at 650°C. Hence, selective sulfation roasting for copper and zinc should be possible at about 600°C. The product is expected to contain $CuSO_4$, $ZnSO_4$, $PbSO_4$, and Fe_2O_3, out of which the last two are insoluble in water.

REFERENCES

1. Moore, J. J. (1990) Chemical Metallurgy, 2nd Edition, Butterworth-Heinemann Ltd., Oxford (Chapter 7).
2. Gilchrist, J. D. (1980) Extraction Metallurgy, 2nd Edition, Pergamon, Oxford (Chapter 12).
3. Rosenqvist, T. (1974) Principles of Extractive Metallurgy, McGraw-Hill, New York (Chapter 8).
4. Coudurier, L., Hopkins, D. W. and Wilkomirski, I. (1978) Fundamentals of Metallurgical Processes, Pergamon, Oxford (Chapter 5).
5. Pehlke, R. D. (1973) Unit Process of Extractive Metallurgy, American Elsevier Pub. Co, New York (Chapter 4).
6. Yazawa, A. (1979) Thermodynamic evaluation of extractive metallurgical processes, Metall. Trans. **10 B**, pp 307–321.
7. Ramakrishna Rao, V. V. V. N. S. and Abraham, K. P. (1971) Kinetics of oxidation of copper sulfide, Metall. Trans. **2 B**, pp 2463–2470.

8. Nagamori, M. and Habashi, F. (1974) Thermodynamic stability of Cu_2SO_4, Metall. Trans. **5 B**, pp 523–524.
9. Ingraham, T. R. and Kellogg, H. H. (1963) Thermodynamic properties of zinc sulfate, zinc basic sulfate and the system Zn-S-O, Trans. Metall. Soc. AIME **227**, pp 1419–1426.
10. Kellogg, H. H. and Basu, S. K. (1960) Thermodynamic properties of the system Pb-S-O, Trans. Metall. Soc. AIME **218**, pp 70–87.
11. Sohn, H. Y. and Goel, R. P. (1979) Principles of roasting, Miner. Sci. Eng. **11** (3), pp 137–153.
12. Turkdogan, E. T. (1980) Physical Chemistry of High Temperature Reactions, Academic Press, New York (Chapter 8).
13. Shamsuddin, M., Ngoc, N. V. and Prasad, P. M. (1990) Sulphation roasting of an off-grade copper concentrate, Met. Mater. Process. **1**, pp 275–292.
14. Ahmadzai, H., Blairs, S., Harris, B. and Staffansson, L. I. (1983) Oxidation aspects of the lime-concentrate pellet roasting process, Metall. Trans. **14B**, pp 589–604.
15. Biswas A. K. and Davenport, D. W. (1976) Extractive Metallurgy of Copper, Elsevier Science Press, New York (Chapter 3).
16. Sommer, A. W. and Kellogg, H. H. (1959) Oxidation of sphalerite by sulfur trioxide, Trans. Metall. Soc. AIME **215**, pp 742–744.
17. Natesan, K. and Philbrook, W. O. (1969) Oxidation kinetic studies of zinc sulfide pellets, Trans. Metall. Soc. AIME **245**, pp 2243–2250.
18. Natesan, K. and Philbrook, W. O. (1970) Oxidation kinetic studies of zinc sulfide in a fluidized bed reactor, Metall. Trans. **1**, pp 1353–1360.
19. Shah, I. D. and Khalafallah, S. E. (1970) Chemical reactions in roasting of copper sulfides, U.S.B.M., RI **7549**, 21 pp.
20. Shah, I. D. and Khalafallah, S. E. (1971) Thermal decomposition of CuS to $Cu_{1.8}S$, Metall. Trans. **2**, pp 605–606.
21. Shah, I. D. and Khalafallah, S. E. (1971) Kinetics and mechanism of the conversion of covellite (CuS) to digenite ($Cu_{1.8}S$), Metall. Trans. **2**, pp 2637–2643.
22. Shah, I. D. and Khalafallah, S. E. (1972) Kinetics of thermal decomposition of copper (II) sulfate and copper (II) oxysulfate, U.S.B.M., RI **7638**, 21 pp.
23. Coudurier, L., Wilkomirski, I. and Morizot, G. (1970) Molybdenite roasting and rhenium volatilization a multiple hearth furnace, Trans. Instn. Min. Metall. **79**, pp C34–40.
24. Amman, P. R. and Loose, T. A. (1971) Oxidation kinetics of molybdenite at 525–635°C, Metall. Trans. **2**, pp 889–893.
25. Khalafallah, S. E. (1979) Roasting as a unit process, In Rate Processes in Extractive Metallurgy, Sohn, H. Y. and Wadsworth, M. E. (Eds.), Plenum Press, New York (Chapter 4, Section 4.1).
26. Ginstling, A. M. and Brounshtein, B. I. J. (1950) The diffusion kinetics of reactions in spherical particles, J. Appl. Chem. USSR **23**, pp 1327–1338.
27. Kubaschewski, O. and Alcock C. B. (1979) Metallurgical Thermochemistry, 5th Edition, Pergamon, Oxford.
28. Curnutt, J. L., Prophet, H., McDonald, R. A. and Syverud, A. N. (1975) JANAF Thermochemical Tables, The Dow Chemical Company, Midland.
29. Barin, I., Knacke, O. and Kubaschewski, O. (1977) Themochemical Properties of Inorganic Substances, (supplement), Springer-Verlag, New York.